# Establishing the impact of food matrix effects on the bioaccessibility of nutraceuticals and pesticides using a standardized food model

| Journal: | *Food & Function* |
|---|---|
| Manuscript ID | FO-ART-11-2018-002368.R1 |
| Article Type: | Paper |
| Date Submitted by the Author: | 23-Jan-2019 |
| Complete List of Authors: | Zhang, Zipei; University of Massachusetts Amherst, Food Science<br>Zhang, Ruojie; University of Massachusetts, Department of Food Science<br>McClements, David; University of Massachusetts, Food Science |
| | |

SCHOLARONE™
Manuscripts

# Establishing the impact of food matrix effects on the bioaccessibility of nutraceuticals and pesticides using a standardized food model

Zipei Zhang[a,1], Ruojie Zhang[a,1], and David Julian McClements[a]*


[a] *Department of Food Science, University of Massachusetts, Amherst, MA 01003, USA*


[1] These authors contributed equally to the present work.

* *Corresponding author:*

D.J. McClements, Department of Food Science, University of Massachusetts, Amherst, MA

01003, USA. Tel.: +1 413-545-2275; fax: +1 413-545-1262; e-mail:

mcclements@foodsci.umass.edu

## Abstract

It is important to establish the impact of food matrix effects on the bioaccessibility of co-ingested substances, such as nutraceuticals, engineered nanomaterials, pharmaceuticals, and pesticides.   Recently,  a standardized food model (SFM) representing a typical US diet has been developed to facilitate these investigations.   This model consists of caseinate-stabilized fat droplets, free casein, pectin, starch, sucrose, and sodium chloride. The SFM was stable to creaming for 2 days, contained small particles ($d \approx 180$ nm), and had a narrow particle size distribution. The SFM was mixed with pureed tomato that had been deliberately contaminated with chlorpyrifos (a hydrophobic pesticide).   The resulting mixture was then exposed to an *in vitro* digestion model. The structural and physicochemical characteristics of the samples (microstructure, particle diameter, and surface potential) were determined after each GIT stage. Also, the bioaccessibility of both chlorpyrifos and lycopene (a hydrophobic nutraceutical) from the pesticide-contaminated tomatoes was determined after the final digestion process.   For lycopene, the bioaccessibility was much lower for tomato alone (0.75%) than for tomato plus SFM (19.0%) (*p < 0.05*).   For chlorpyrifos, the bioaccessibility was also appreciably lower for tomato alone (40.4%) than for tomato plus SFM (58.7%), but the effect was less dramatic (*p < 0.05*). Our results indicate that a standardized food matrix impacts the bioaccessibility of hydrophobic bioactives in fresh produce by an amount that depends on the nature of the bioactive agent. The SFM developed here may therefore be useful for screening the potential impact of food matrix effects on the bioaccessibility of ingested bioactives and other substances.

## Introduction

An increasing number of researchers are focusing on the impact of foods on the uptake of bioactive substances ingested at the same time as them, such as drugs, nutraceuticals, pesticides, and nanoparticles. [1-5] The nature of the food matrix impacts the bioavailability of these bioactive substances by modifying their bioaccessibility, absorption, or transformation within the human gastrointestinal tract (GIT). [6-8] Scientists are therefore trying to understand and control these effects so they can improve the efficacy of drugs and nutraceuticals or reduce the potential toxicity of pesticides and nanomaterials. [9-11] In general, food matrix effects depend on the chemical constituents within the foodstuff, such as fats, proteins, carbohydrates, minerals and various other components, as well as the way these constituents are structurally organized. [12, 13] In turn, the characteristics of the food matrix influence the structure and composition of the gastrointestinal fluids surrounding the co-ingested bioactive substances, thereby influencing their solubility, metabolism, and uptake. [14-16] An understanding of food matrix effects is therefore essential for predicting the gastrointestinal behavior of both beneficial and harmful bioactive substances in our diet.

For this reason, there is an impetus to include food matrix effects in studies of the factors influencing the bioavailability of bioactive substances. Various approaches can be utilized to achieve this goal. Researchers can study the impact of real foods, such as milk, meat, or bread, on the bioavailability of specific bioactive substances. This approach is useful when the bioactive substance is known to regularly occur within a particular type of food, such as titanium

dioxide in chewing gum or vitamin D in milk. [17, 18]   There are, however, some limitations to this

approach.   Some bioactives are ingested as part of complex diets containing many kinds of

foods and their gastrointestinal fate is determined by the precise features of the food matrix

employed. [19]   Moreover, there are often substantial variations in the composition and structure

of specific foods from batch-to-batch, making reproducibility more difficult. [20]   These

limitations probably account for many of the conflicting results reported in the literature about

the impact of food matrix effects on the bioaccessibility or bioavailability of bioactive substances

when different whole foods are used. [5, 12, 21]

An alternative approach is to develop a standardized food model (SFM) to serve as a

representative of a broad category of different foods.   In general, foods are structurally complex

multicomponent materials containing various types and levels of carbohydrates, fats, proteins,

minerals, water, and other components. [22, 23]   It would, therefore, be beneficial to have an SFM

with a harmonized composition and structure that could be used by researchers in different

laboratories to test food matrix effects.   This model would allow researchers to obtain

reproducible results under standardized conditions, thereby leading to an improved systematic

understanding of the influence of the food matrix on oral bioavailability of different bioactive

agents.   It may then be possible to establish general trends between bioactive type and the

magnitude of food matrix effects.

The purpose of the current study was to test a newly developed standardized food model

(SFM) for including food matrix effects in *in vitro* bioaccessibility studies [24].   This SFM was

designed to mimic the nutrient composition of a representative US diet and includes appropriate

levels of representative fats, digestible carbohydrates, dietary fibers, proteins, and minerals.   We

studied the impact of the SFM on the bioaccessibility of two bioactive substances, one beneficial

(carotenoids) and one detrimental (pesticides) to health.   Produce, such as vegetables and fruits,

are often consumed with other foods.   For instance, raw or cooked tomatoes may be eaten with a

salad dressing or a cooking sauce.   To our knowledge, this is the first study on the influence of

food matrix effects on the bioaccessibility of both nutraceuticals and pesticides from the same

fresh produce.   We investigated the impact of the SFM on the bioaccessibility of a hydrophobic

nutraceutical (lycopene) and hydrophobic pesticide (choripyrifos) in raw tomatoes using a static

simulated gastrointestinal tract (GIT) that mimics the human mouth, stomach, and small

intestine.

The utilization of this standardized food model should help to elucidate those bioactive

substances that are most susceptible to food matrix effects, *i.e.,* whose bioaccessibility may be

strongly influenced by the major components in foods.   Once identified, further studies could be

carried out to identify which food components are most important in influencing their

bioaccessibility.

## Materials and Methods

### Materials

Corn oil and fresh tomatoes were obtained from a supermarket. Sodium chloride and sucrose

were obtained from the Fisher Chemical Company (Pittsburgh, PA).   Modified food starch was

obtained from the Grain Processing Corporation (Muscatine, IA). Pectin was obtained from TIC

GUMs (White Marsh, MD). Sodium caseinate was obtained from the American Casein Company

(MP Biomedicals LLC). Scintiverse cocktail was obtained from PerkinElmer (PerkinElmer, Inc.,

Walthanm, MA). Radioactive-labeled [$^{14}$C] chlorpyrifos was obtained from Dow AgroSciences

LLC (Indianapolis, IN) and the manufacturer reports that it has specific activity around 26.8

mCi/mmol. The following chemicals were obtained from the Sigma-Aldrich Chemical Company

(St Louis, MO): pepsin from porcine gastric mucosa (250 units per mg); pancreatin (100–400

units per mg protein); mucin from porcine stomach; lycopene standard; porcine bile extract;

unlabeled chlorpyrifos and Nile red. All solutions were prepared using double distilled water.

**Standardized food model preparation**

The initial development of the SFM used in the current study was described in detail in our

recent publication.[24]   The proportion of nutrients in a typical US diet was obtained from the

"What We Eat in America" database (NHANES 2013-2014) maintained by the Harvard School

of Public Health (www.ars.usda.gov).   The nutrients contained in the SFM are summarized in

**Table 1**.   A summary of the protocol used to produce 100 g of SFM is described below:

(I)     *Emulsion preparation*: Sodium caseinate (1%, w/w) was dissolved in phosphate

buffer solution (10 mM, pH 7) by continual stirring for 2 hours at ambient

temperature. The resulting caseinate solution was then filtered to remove any

residual insoluble matter. After adding corn oil (7.64%, w/w), the mixture was

blended for 2 minutes using a high shear mixer (M133/1281-0, Biospec Products,

Inc., ESGC, Switzerland). This emulsion was then passed through a microfluidizer

(M110Y, Microfluidics, Newton, MA) three-times at a pressure of 82.7 MPa to create an emulsion containing small lipid droplets.

(II)     *Protein addition*: Powdered sodium caseinate was gradually poured into this emulsion to reach a final concentration of 7.68% w/w protein. The mixture solution was continuously stirred around 30 min to ensure the total dissolution.

(III)    *Pectin addition*: An aqueous pectin (1.56% w/v) solution was obtained by dispersing pectin powder into distilled water and then mixing at 50 °C for 60 min. The mixture was then reduced to room temperature and stirred continuously to fully dissolve the pectin. Then 44.8g of the prepared pectin solution was mixed with 44.8 g of emulsion (1:1, w/w).

(IV)    *Starch addition*: 5.15 g of corn starch was slowly poured into the previous mixture with continuous stirring until it was fully dissolved (around 30 min).

(V)     *Sucrose addition*: 4.57 g of sucrose was slowly poured into the previous mixture with continuous stirring until it was fully dissolved (around 10 min).

(VI)    *Salt addition*: 0.534g of sodium chloride was slowly poured into the previous mixture with continuous stirring until it was fully dissolved (around 30 min). The speed of stirring should be high enough to induce uniform stirring and it may be increased when the viscosity increased caused by chemicals addition.

(VII)   *SFM powder preparation*: To facilitate storage, spray drying was used to convert the SFM solution from a fluid to a powder.   The fluid SFM sample was spray dried at a feed rate of 0.45 L/h at 170 °C inlet temperature using a spray-drier (Mini spray-dryer B-290, Büchi, Switzerland) with a 0.7 mm nozzle atomizer. The resulting powders were stored in hermetically sealed vessels at 4 °C. It should be noted that the fluid form of the SFM was used for all the experiments except specific in current study.

(VIII) *SFM reconstitution*:   The powdered SFM was changed back to a fluid form utilizing

the following procedure.   To prepare 100g of fluid SFM, powdered SFM (17.8 g)

was gradually poured into double distilled water (82.2g) with continuous stirring

using a magnetic stirring device.   Stirring was carried out at ambient temperature for

at least 30 min to ensure full dissolution of the powder.

In this model, the pectin, starch, and sucrose were used to represent the carbohydrates,

sodium caseinate the proteins, corn oil the fat, and sodium chloride the minerals.

**Chlorpyrifos standard solution preparation**

A standard pesticide solution of known concentration was prepared by dissolving either

unlabeled or radio-labeled [$^{14}$C] chlorpyrifos in acetonitrile to reach a final concentration of 50

ppm.

**Preparation of pesticide-contaminated tomatoes**

Fresh tomatoes were sliced into small cubes and then blended by using a high-shear blender

for 1 min to disrupt the tomato tissue. The resulting tomato puree (10 g) were mixed with [$^{14}$C]

chlorpyrifos or unlabeled chlorpyrifos standard solution (100 μL) to obtain a final pesticide level

of 0.5 ppm, which is the permitted maximum residue (MRL) level for chlorpyrifos. [25]

Similar amounts of pesticide-contaminated tomato sample were then mixed with either fluid

SFM (sample) or phosphate buffer (control). [26]

**GIT model**

Mixtures of SFM and chlorpyrifos-treated tomatoes were subjected to a simulated GIT that

mimics the mouth, stomach, and small intestine.   This model was adopted from the one

described in our recent study with some modifications. [5, 26]　A brief summary of the model is

given below.

*Initial system*: 20 g of SFM was poured into a glass beaker and then swirled using a

temperature-controlled shaking device (37 °C) set at 100 rpm for 15 min to warm up the samples

(Innova Incubator Shaker, Model 4080, New Brunswick Scientific, Edison, NJ).

*Mouth stage*: A simulated saliva fluid (SSF) was prepared that contained mucin (0.003

g/mL) and amylase (150 units/mL), which was pre-heated to 37 °C after adjusting the pH to 6.8.

[27-29]　Then, a portion of the sample from the initial system (20.0 g) was mixed with an equal

amount of SSF (20 g) with continual stirring. The system was re-adjusted to pH 6.8 followed by

swirling in the temperature-controlled shaking device (37 °C) for 2 min to mimic agitation in the

mouth.

*Gastric stage*: A simulated gastric fluid (SGF) that contained pepsin (0.0032 g/mL) was

prepared and then heated to 37 °C.　Then, a portion of the sample from the mouth stage (20.0 g)

was mixed with SGF solution (20.0g) and then the resulting mixture was adjusted to pH 2.5. The

mixture was then placed in the temperature-controlled shaking device (37 °C) for 2 h to mimic

the stomach phase.

*Small intestine stage*: A portion of the sample from the gastric stage (30.0 g) was poured

into a glass beaker that had been incubated at 37 °C in a water bath. The obtained samples were

adjusted to pH 7.00 with continuous stirring (600 rpm). An aliquot (1.5 mL) of simulated

intestinal fluid (mixture of NaCl and $CaCl_2$) and then an aliquot (3.5 mL) of bile salt solution

were then added to the glass beaker with continuous stirring. After the mixture in the reaction

vessel had been adjusted back to pH 7.00, pancreatin solution (2.5 mL) was added to the mixture.

The amounts of $CaCl_2$, NaCl, pancreatin and bile salts in the final system were 10.0 mM, 150

mM, 2.4 mg/mL and 5.0 mg/mL, respectively. The pH of the final system was monitored and

adjusted using an automatic titration system (Metrohm, USA Inc.). The volume of alkaline

solution (NaOH) titrated into the samples to neutralize the free fatty acids (FFAs) generated by

lipid digestion was measured, and then the extent of lipid digestion was determined from the

titration curves as described previously. [30]

It should be noted that the model used in our study is closely related to the standardized

INFOGEST model that has recently been adopted by many laboratories. [31, 32] However, our

model includes a mouth phase and is optimized for the study of emulsion-based foods. The

main differences between our model and the INFOGEST one are the precise levels of enzymes,

minerals, and other gastrointestinal components included. It should be noted that gastric lipase

was not included in our study due to the difficulties in obtaining an affordable and reliable

source, but this may be important for future studies since it is known that lipid digestion is

initiated in the stomach [33].

The physicochemical properties of the samples were determined after each digestion stage

based on the methods described in the following sections. The bioaccessibility of lycopene and

chlorpyrifos were determined after the end of intestinal digestion stage.

**Determination of particle characteristics**

The properties of the colloidal particles present within the tomato-SFM systems were determined after they being exposed to the different stages of the GIT model. Particle size distributions were determined using laser diffraction (Mastersizer 2000, Malvern Instruments Ltd., Malvern, Worcestershire, UK). Surface potentials ($\zeta$-potential) were measured using particle electrophoresis (Zetasizer Nano ZA series, Malvern Instruments Ltd. Worcestershire, UK). The refractive indices of the dispersed and continuous phases used in the mathematical models were 1.47 and 1.33 for the calculation of particle size and surface potential.

To minimize errors caused by multiple scattering, the initial, mouth, and small intestine samples were diluted using phosphate buffer (5 mM, pH 7.0) and the stomach samples was diluted using acidified water (pH 2.5). It should be noted that the mathematical model employed for interpretation of the light scattering data is based on the assumption that the scattering entities are spherical particles with uniform refractive indices. Obviously, this will not be the case for tomato tissues or highly flocculated droplets and so the data should be treated with caution and only used to provide a rough indication.

The microstructure of SFM was studied by using a confocal laser scanning microscopy (Nikon D-Eclipse C1 80i, Nikon, Melville, NY, U.S.) with a 40 × objective lens. The oil phase was dyed using Nile red solution (1mg/mL ethanol) to facilitate the observation. The wavelengths used to excite and detect the hydrophobic dye (Nile Red) within the samples were

543 nm and 605 nm, respectively.   Images of all samples were acquired and stored using image

analysis software (NIS-Elements, Nikon, Melville, NY). [26]

**Bioaccessibility measurements**

The bioaccessibilities of lycopene and chlorpyrifos were determined after each sample had

gone through the entire GIT model as described previously. [34, 35]   At the completion of the small

intestine stage, the "digest" obtained was subjected to centrifugation at 18,000 rpm (4 °C for 50

min).   The bioaccessibility was determined from the lycopene or chlorpyrifos concentrations

measured in the mixed micelle fraction and in the overall digest:

$$Bioaccessibility\ (\%) = 100\ \times \frac{C_{Micelle}}{C_{Digest}}$$

Here, $C_{micelle}$ and $C_{Digest}$ are the concentrations of the bioactive substance in the mixed micelle

phase and in the overall digest, respectively. The same procedure was utilized for both the

pesticide and lycopene determination.

**Chlorpyrifos and lycopene determination**

The magnitude of the $^{14}$C-radioactive signal in the samples were measured by a liquid

scintillation counting method (Bechman LS6500) to indicate the concentration of chlorpyrifos.

The lycopene concentration was determined by HPLC.   The analytical methods used have been

described in detail elsewhere and therefore are not listed here. [26, 36]

**Statistical analyses**

Three or more newly prepared samples were used for each measurement and the results

were analyzed using specialized statistical software (SPSS) and Excel (Microsoft, Redmond,

VA, USA). The difference between means was calculated by a Duncan's multiple range tests with a confidence level of 95%.

## Results and Discussion

### Standardized food model preparation and characterization

In the current study, our intention was to examine the impact of a recently developed standardized food model (SFM) [24] on the gastrointestinal fate of two co-ingested bioactive substances – a nutraceutical and a pesticide. These two bioactive substances were present within the same fresh product (pureed tomato).

Initially, we characterized the properties of the fluid SFM used in this study. Visual observations indicated that the SFM samples were opaque white fluids with a uniform appearance that showed no evidence of phase separation during two days storage at ambient temperature. Light scattering measurements showed that the SFM contained a single population of relatively small particles with diameters centered around 180 nm (**Figure 1b**), which were attributed to the fat droplets. Collectively, our results suggest the fat droplets in the SFM were fairly small and had good stability against irreversible aggregation and creaming.

The high stability of the SFM may have been because that the protein-coated fat droplets (-24.6 mV, **Figure 2**), non-adsorbed proteins, and pectin molecules [37] were all highly anionic at neutral pH, leading to an intense electrostatic repulsion amongst them. [38]

**Particle characterization during gastrointestinal passage**

In this series of experiments, alterations in the particle characteristics within the three types

of sample were detected after they passing through the simulated GIT: (i) crushed tomatoes; (ii)

SFM; (iii) crushed tomatoes + SFM.

*Charge properties*

*Initial Samples:* The $\zeta$-potentials of all the initial samples were negative: -26.8, -24.8 and -

12.5 mV for crushed tomatoes, SFM, and crushed tomatoes + SFM samples, respectively

(**Figure 2**).   The negative charge of the SFM samples should be due to the presence of anionic

polymers and particles, such as casein-coated oil droplets and pectin molecules, as discussed

earlier.   The anionic nature on the crushed tomato may be attributed to negatively charged

biopolymers (e.g., pectin) associated with the tomato fragments. [39]   Surprisingly, the magnitude

of the negative surface potential on the particles within the mixed systems was much less than

within the individual systems (*p < 0.05*).   One possible explanation is that some of the

constituents released from the tomato fragments, like organic acids, mineral ions, or charged

biopolymers, accumulated around or bound to protein-coated fat droplet surfaces within the

SFM.   As a result, the $\zeta$-potential of the fat droplets was changed, due to an alteration in either

their surface charge density or the ionic composition of the surrounding solution. This result

agrees with our earlier study, which also found the magnitude of the negative charge on WPI-

coated fat droplets became smaller after they were incubated with tomato tissue. [39]

*Mouth phase:* After exposure to simulated oral conditions, we observed a small reduction in the magnitude of the negative charge for both the crushed tomato and SFM samples.   This change might be a result of ion binding and/or electrostatic screening associated with the mineral ions and mucin molecules in the artificial saliva. [40]   Conversely, the magnitude of the negative particle charge in the mixed systems increased substantially ($p < 0.05$) after they had been exposed to the simulated oral conditions, so that it became much more similar to that in the tomato only and SFM only samples (**Figure 2**).   The cause of this effect is not known at present. One possibility is that the mucin molecules bound to some of the ions or polymers released from the tomato fragments, thereby reducing their tendency to interact with the fat droplets. Further studies, however, are required to establish the cause of this phenomenon.

*Stomach phase:* There was an appreciable reduction ($p < 0.05$) in the magnitude of the negative particle charge for all three samples after incubation in the simulated stomach (**Figure 2**).   This observed change in electrical characteristics is probably due to the highly acid nature of the gastric fluids.   Pectin loses most of its anionic character in acidic environments because of protonation of its carboxyl groups (pKa = 3.5). [41]   For the crushed tomatoes, the low pH of the gastric fluids would also have led to the protonation of any anionic biopolymers naturally present within the plant tissue, such as pectin.   For the SFM samples, the casein-coated fat droplets are expected to be highly cationic under the strongly acidic gastric conditions because this protein has an isoelectric point around pH 4.6.   In practice, they were slightly anionic, which suggests that negatively charged mucin, pectin, or chloride ions absorbed to their surfaces.   Moreover,

the magnitude of the surface potential should decrease because of electrostatic screening linked

to the mineral ions within the gastric fluids.   Presumably, similar effects occurred in the mixed

systems.

*Small intestine phase:*   The particles in the samples were all strongly negatively charged by

completion of the small intestine stage (**Figure 2**).   As reported previously, this effect is because

the digested samples contain various anionic species that contribute to the measured signal,

including bile acids, free fatty acids, phospholipids, non-digested proteins, peptides, pectin, and

mucin. [42]   These anionic species may have been part of colloidal particles or polymers

sufficiently large to scatter light waves and so contribute to the electrophoretic signal used for

the calculation of the $\zeta$-potential.

*Particle size and microstructure*

The particle size distribution (PSD) and microstructure of the samples were measured using

laser diffraction (**Figure 1**) and confocal microscopy (**Figure 3**), respectively.   Only the samples

containing fats were analyzed by confocal microscopy because a fluorescence dye (Nile red) was

employed to visualize them.   In a recent study using optical microscopy, we found that the

tomato fragments remained intact throughout the GIT [43].

*Crushed tomatoes:*   For the crushed tomatoes, the overall shape of the PSD stayed fairly

similar after passing through different stage in GIT (**Figure 1a**).   These samples contained a

population of relatively large particles (100–1000 μm) that appeared to be resistant to disruption

or aggregation under GIT conditions. Presumably, these particles were fragments of tomato tissue that contained dietary fibers resistant to acid hydrolysis, enzymatic digestion, and physical disruption.

*SFM samples*: The PSDs showed the SFM samples initially contained a population of fairly small particles (**Figure 1b**), presumably casein-coated fat droplets. Interestingly, microscopy analysis showed there was a substantial amount of flocculation in these initial samples (**Figure 3**), even though particle size analysis by laser diffraction showed that the individual fat droplets were still fairly small. This suggests that the fat droplets in the initial samples had gathered into flocs kept together by weak attractive interactions. These flocs were broken down when the samples were diluted and stirred for the laser diffraction analysis. Previous studies have suggested that this effect was due to depletion flocculation induced because of the high level of non-adsorbed biopolymers in the continuous phase of the SFM. [37, 44] There was not a major change in the measured PSD after the SFM samples had been exposed to the mouth stage, which suggested that the fat droplets remained fairly stable to strong aggregation. Moreover, the microscopy analysis indicated that the fat droplets were no longer flocculated after being exposed to the mouth phase. This may have been because the initial samples had been diluted, which reduced the level of non-adsorbed polymers in the continuous phase, and therefore reduced the magnitude of the depletion attraction between the fat droplets. [45]

After being exposed to the simulated stomach, a large rise in the size of the particles in the SFM samples was observed in both the light scattering (**Figure 1b**) and microscopy (**Figure 3**)

results.   This result suggests that the lipid droplets had become strongly associated with each other.   The most likely reasons for this phenomenon are bridging flocculation induced by the cationic protein-coated fat droplets with anionic mucin and pectin molecules.   In addition, there will have been a decrease in the electrostatic repulsion amongst the particles because of the reduction in their surface potential and the rise in ionic strength of the gastric fluids.

Microscopy analysis showed there was an appreciable decrease in the size of the lipid-rich aggregates in the SFM samples after incubation within the small intestine (**Figure 3**), while the light scattering measurements suggested that some large particles still remained (**Figure 1b**). These results suggest that most of the fat droplets were hydrolyzed by lipase in the small intestine, leading to the formation of a range of differently-sized lipid-rich particles, such as vesicles, calcium soaps, and partially digested fat droplets.

*Mixed systems:* The mixed systems, which contained both crushed tomato and SMF, exhibited some characteristics similar to those exhibited by the two individual components (**Figures 1c and 3**).   The light scattering measurements showed that the mixed systems contained a population of large particles, presumably tomato fragments, which remained relatively intact throughout the simulated GIT (**Figure 1c**).   Furthermore, there was some evidence of a population of smaller particles, which were probably the fat droplets.   The microscopy analysis showed that the fat droplets in the SFM and mixed systems behaved very similarly (**Figure 3**).   They were highly flocculated initially, became evenly dispersed in the mouth, aggregated in the stomach, and were finally hydrolyzed in the small intestine.   These

results suggest that the presence of the tomato fragments does not have a major impact on the gastrointestinal fate of the fat droplets.

**Lipid digestion**

Lipids are one of the main constituents (3.42%) of the SFM and their digestion is known to have an important impact on the bioaccessibility of hydrophobic bioactive substances. [15]   It is therefore important to measure the lipid digestion profiles of the SFM to facilitate the interpretation of the bioaccessibility data.   This was carried out using an automatic titrator that monitors lipid hydrolysis throughout the duration of the small intestine stage.   The volume of NaOH solution needed to neutralize the generated free fatty acids (FFAs) after lipase was added to the samples was measured, and then transformed into the fraction of lipids digestion as described earlier (**Figure 4)**.

For the crushed tomato, only a small rise in the volume of consumed alkaline solution occurred during the 2 h digestion period.   This may have been a result of the digestion of some of the components within the gastrointestinal fluids (such as lipase or bile salts) or due to organic acids released from the tomato tissues during digestion. [39]   For the SFM, there was a sharp rise in generated FFAs during the first 10 min of digestion, followed by a slower rise at longer incubation times.   Surprisingly, the calculated amount of FFAs released at the end of digestion (120%) was appreciably higher than the expected value (100%).   This may have been because there were other non-fat components in the SFM that were also digested by the simulated pancreatic juices, such as proteins and starches. [46, 47]   For the mixed system, which consisted of

crushed tomatoes and SFM, the overall shape of the digestion profile was fairly similar to that of

the SFM system.   However, the final level of FFAs released was appreciably lower (96%) by

the completion of the small intestine stage.   This result indicates that the presence of the tomato

tissue inhibited the digestion of some of the components in the SFM samples.   For instance,

proteins, starches, or lipid droplets may have been trapped in the tomato tissues because of

capillary forces associated with the tiny pores within the plant tissues or because of binding to

the plant tissues. [39]   As a result, the ability of the digestive enzymes to access these components

was reduced, slowing down digestion.   Alternatively, the presence of the tomato tissues may

have altered the viscosity of the GIT fluids, thereby slowing down the movement of the enzymes

and substrates, as has been suggested in previous studies [48].   Clearly, further studies are required

in the future to identity the precise physicochemical phenomena involved.

**Bioaccessibility of chlorpyrifos and lycopene**

In this series of experiments, the impact of food matrix effects on lycopene and chlorpyrifos

bioaccessibility in pesticide-contaminated tomatoes was investigated in the absence (control) and

presence of SFM.   The bioaccessibility was assumed to be the percentage of the bioactive

substances in the total digest that ended up inside the mixed micelles at the completion of the

small intestine stage. [26]

The bioaccessibility of lycopene in the control samples was extremely low (0.75%) (**Figure**

**5**), which was probably because of the lack of digestible fat in this sample.   As a result, there

were no mixed micelles generated that able to solubilize the lycopene molecules released from

the tomato fragments during digestion. [49]    Instead, the lycopene molecules would tend to form crystals in the aqueous phase that precipitated to the bottom of the digest.    Conversely, the bioaccessibility of lycopene in the tomato samples mixed with SFM was much higher (19.0%) ($p < 0.05$).   This phenomenon is likely a result of solubilization of the lycopene in the mixed micelles generated when the fat in the SFM was digested by lipase.   This result clearly demonstrates that there is a very strong food matrix effect for lycopene. [50]

In contrast, the bioaccessibility of chlorpyrifos in the presence of SFM (58.7%) was only slightly higher than in its absence (40.4%) ($p < 0.05$).   This is probably because chlorpyrifos is a much smaller molecule ($M_w$ = 351 g/mol) with a lower affinity for oil (LogP = 4.8) and a higher water solubility (1.1 mg/L) than lycopene.   In the current research, some of this pesticide may have been solubilized directly within the aqueous phase at the low levels of chlorpyrifos (0.05 mg/L) present in the small intestinal fluids. Furthermore, the simple micelles could be formed from bile salts in the simulated small intestine fluids, which may also have solubilized a fraction of the small chlorpyrifos molecules.   This was not the case with lycopene because the hydrophobic interiors of the simple micelles were too small to accommodate the large non-polar carotenoid molecules. [36]

## Conclusion

In this study, we have shown that a recently developed standardized food model can be utilized to investigated the influence of food matrix effects on the bioaccessibility of hydrophobic bioactive substances.   The SFM was mixed with chlorpyrifos-contaminated tomato

puree to investigate the influence of food matrix effects on the bioaccessibility of both a pesticide (chlorpyrifos) and a nutraceutical (lycopene) in the same system. The simulated gastrointestinal studies showed that most of the lipids in the SFM had been digested by the completion of the small intestine stage. The mixing of the SFM with chlorpyrifos-contaminated tomatoes increased the bioaccessibility of chlorpyrifos somewhat (from 40.4% to 58.7%, *i.e.,* 1.5-fold) but greatly increased the bioaccessibility of lycopene (from 0.75% to 19.0%, *i.e.,* 25-fold). This result highlights that there are major differences between the impact of food matrix effects on different bioactive substances, which may be due to differences in their liberation from the plant tissues and incorporation into the mixed micelles.

Overall, we believe that this standardized food model is useful for providing information about the potential impact of food matrix effects on the bioaccessibility of different bioactive substances. In particular, the availability of an SFM could lead to more reproducible measurements and ease the critical evaluation of results from different laboratories. Even so, it should be stressed that this is a highly simplistic food model that cannot account for the diverse compositions, structures, and physicochemical properties of real foods. Despite these limitations, the SFM does provide a useful screening tool to highlight the susceptibility of different bioactive substances to food matrix effects. Once the importance of food matrix effects has been identified for a particular bioactive agent, researchers could carry out more detailed studies to determine their precise origin.

## Acknowledgements

# References

1.  M. Yang, S. I Koo, W. O Song and O. J. C. m. c. K Chun, Food matrix affecting anthocyanin bioavailability, 2011, **18**, 291-300.

2.  D. M. Ribnicky, D. E. Roopchand, A. Oren, M. Grace, A. Poulev, M. A. Lila, R. Havenaar and I. J. F. c. Raskin, Effects of a high fat meal matrix and protein complexation on the bioaccessibility of blueberry anthocyanins using the TNO gastrointestinal model (TIM-1), 2014, **142**, 349-357.

3.  H. Sengul, E. Surek and D. J. F. R. I. Nilufer-Erdil, Investigating the effects of food matrix and food components on bioaccessibility of pomegranate (Punica granatum) phenolics and anthocyanins using an in-vitro gastrointestinal digestion model, 2014, **62**, 1069-1079.

4.  R. D. Toothaker, P. G. J. A. R. o. P. Welling and Toxicology, The effect of food on drug bioavailability, 1980, **20**, 173-199.

5.  G. M. DeLoid, Y. Wang, K. Kapronezai, L. R. Lorente, R. Zhang, G. Pyrgiotakis, N. V. Konduru, M. Ericsson, J. C. White and R. De La Torre-Roche, An integrated methodology for assessing the impact of food matrix and gastrointestinal effects on the biokinetics and cellular toxicity of ingested engineered nanomaterials, *Particle and fibre toxicology*, 2017, **14**, 40.

6.  A. Serra, A. Macia, M.-P. Romero, J. Valls, C. Bladé, L. Arola and M.-J. Motilva, Bioavailability of procyanidin dimers and trimers and matrix food effects in in vitro and in vivo models, *British Journal of Nutrition*, 2010, **103**, 944-952.

7.  M. Kataoka, Y. Masaoka, S. Sakuma and S. Yamashita, Effect of food intake on the oral absorption of poorly water-soluble drugs: in vitro assessment of drug dissolution and permeation assay system, *Journal of Pharmaceutical Sciences*, 2006, **95**, 2051-2061.

8.  M. J. Rodríguez-Roque, B. de Ancos, C. Sánchez-Moreno, M. P. Cano, P. Elez-Martínez and O. Martín-Belloso, Impact of food matrix and processing on the in vitro bioaccessibility of vitamin C, phenolic compounds, and hydrophilic antioxidant activity from fruit juice-based beverages, *Journal of Functional Foods*, 2015, **14**, 33-43.

9.  R. Bushra, N. Aslam and A. Y. Khan, Food-drug interactions, *Oman Medical Journal*, 2011, **26**, 77.

10. B. SandstroÈm, Micronutrient interactions: effects on absorption and bioavailability, *British Journal of Nutrition*, 2001, **85**, S181-S185.

11. Y. M. Jeanes, W. L. Hall, S. Ellard, E. Lee and J. K. Lodge, The absorption of vitamin E is influenced by the amount of fat in a meal and the food matrix, *British Journal of Nutrition*, 2004, **92**, 575-579.

12. E. Capuano, T. Oliviero and M. A. J. S. van Boekel, Modeling food matrix effects on chemical reactivity: Challenges and perspectives, *Critical Teviews in Food Science and Nutrition*, 2017, 1-15.

13. R. W. G. van Willige, J. P. H. Linssen and A. G. J. Voragen, Influence of food matrix on absorption of flavour compounds by linear low-density polyethylene: proteins and carbohydrates, *Journal of the Science of Food and Agriculture*, 2000, **80**, 1779-1789.

14. Z. Guo, N. J. Martucci, F. Moreno-Olivas, E. Tako and G. J. Mahler, Titanium dioxide nanoparticle ingestion alters nutrient absorption in an in vitro model of the small intestine, *NanoImpact*, 2017, **5**, 70-82.

15. M. Yao, D. J. McClements, F. Zhao, R. W. Craig and H. Xiao, Controlling the gastrointestinal fate of nutraceutical and pharmaceutical-enriched lipid nanoparticles: From mixed micelles to chylomicrons, *NanoImpact*, 2017, **5**, 13-21.

16. P. G. Welling, Effects of food on drug absorption, *Annual Review of Nutrition*, 1996, **16**, 383-415.

17. X. X. Chen, B. Cheng, Y. X. Yang, A. Cao, J. H. Liu, L. J. Du, Y. Liu, Y. Zhao and H. Wang, Characterization and preliminary toxicity assay of nano-titanium dioxide additive in sugar-coated chewing gum, *Small*, 2013, **9**, 1765-1774.

18. J. Senterre, G. Putet, B. Salle and J. Rigo, Effects of vitamin D and phosphorus supplementation on calcium retention in preterm infants fed banked human milk, *Journal of Pediatrics*, 1983.

19. M. C. Walton, W. H. Hendriks, A. M. Broomfield and T. K. McGhie, Viscous food matrix influences absorption and excretion but not metabolism of blackcurrant anthocyanins in rats, *Journal of Food Science*, 2009, **74**, H22-H29.

20. J. Ubbink, A. Burbidge and R. Mezzenga, Food structure and functionality: a soft matter perspective, *Soft Matter*, 2008, **4**, 1569-1581.

21. P. Šimon and E. Joner, Conceivable interactions of biopersistent nanoparticles with food matrix and living systems following from their physicochemical properties, *Journal of Food & Nutrition Research*, 2008, **47**.

22. D. J. McClements and H. Xiao, Is nano safe in foods? Establishing the factors impacting the gastrointestinal fate and toxicity of organic and inorganic food-grade nanoparticles, *npj Science of Food*, 2017, **1**, 6.

23. C. Wilkinson, G. B. Dijksterhuis and M. Minekus, From food structure to texture, *Trends in Food Science & Technology*, 2000, **11**, 442-450.

24. Z. Zhang, R. Zhang, H. Xiao, K. Bhattacharya, D. Bitounis, P. Demokritou and D. J. McClements, Development of a standardized food model for studying the impact of food

matrix effects on the gastrointestinal fate and toxicity of ingested nanomaterials, *NanoImpact*, 2019, **13**, 13-25.

25. P. Aysal, K. Gözek, N. Artık and A. S. Tuncbilek, 14 C-Chlorpyrifos Residues in Tomatoes and Tomato Products, *Bulletin of environmental contamination and toxicology*, 1999, **62**, 377-382.

26. R. Zhang, W. Wu, Z. Zhang, Y. Park, L. He, B. Xing and D. J. McClements, Effect of the Composition and Structure of Excipient Emulsion on the Bioaccessibility of Pesticide Residue in Agricultural Products, *Journal of Agricultural and Food Chemistry*, 2017, **65**, 9128-9138.

27. P. Kapsimalis, S. L. Rosenthal, W. Updegrave, R. Evans, B. Hurley and H. M. Cobe, The relationship between caries activity, flow rate, total nitrogen and the mucin content of saliva, *Journal of Oral Medicine*, 1966, **21**, 107-110.

28. F. Q. Ionta, F. L. Mendonça, G. C. de Oliveira, C. R. B. de Alencar, H. M. Honorio, A. C. Magalhaes and D. Rios, In vitro assessment of artificial saliva formulations on initial enamel erosion remineralization, *Journal of Dentistry*, 2014, **42**, 175-179.

29. R. Zhang and D. J. McClements, in *Nanoemulsions*, Elsevier, 2018, pp. 577-612.

30. Y. Li and D. J. McClements, New mathematical model for interpreting pH-stat digestion profiles: Impact of lipid droplet characteristics on in vitro digestibility, *Journal of Agricultural and Food Chemistry*, 2010, **58**, 8085-8092.

31. M. Minekus, M. Alminger, P. Alvito, S. Ballance, T. Bohn, C. Bourlieu, F. Carriere, R. Boutrou, M. Corredig and D. Dupont, A standardised static in vitro digestion method suitable for food–an international consensus, *Food & Function*, 2014, **5**, 1113-1124.

32. S. N. El, S. Karakaya, S. Simsek, D. Dupont, E. Menfaatli and A. T. Eker, In vitro digestibility of goat milk and kefir with a new standardised static digestion method (INFOGEST cost action) and bioactivities of the resultant peptides, *Food & Function*, 2015, **6**, 2322-2330.

33. M. Koziolek, F. Carriere and C. J. H. Porter, Lipids in the Stomach - Implications for the Evaluation of Food Effects on Oral Drug Absorption, *Pharmaceutical Research*, 2018, **35**.

34. C. Qian, E. A. Decker, H. Xiao and D. J. McClements, Nanoemulsion delivery systems: influence of carrier oil on β-carotene bioaccessibility, *Food Chemistry*, 2012, **135**, 1440-1447.

35. L. Salvia-Trujillo, C. Qian, O. Martín-Belloso and D. J. McClements, Influence of particle size on lipid digestion and β-carotene bioaccessibility in emulsions and nanoemulsions, *Food Chemistry*, 2013, **141**, 1472-1480.

36. R. Zhang, Z. Zhang, L. Zou, H. Xiao, G. Zhang, E. A. Decker and D. J. McClements, Enhancing nutraceutical bioavailability from raw and cooked vegetables using excipient emulsions: influence of lipid type on carotenoid bioaccessibility from carrots, *Journal of Agricultural and Food Chemistry*, 2015, **63**, 10508-10517.

37. J. Surh, E. A. Decker and D. J. McClements, Influence of pH and pectin type on properties and stability of sodium-caseinate stabilized oil-in-water emulsions, *Food Hydrocolloids*, 2006, **20**, 607-618.

38. L. Jourdain, M. E. Leser, C. Schmitt, M. Michel and E. Dickinson, Stability of emulsions containing sodium caseinate and dextran sulfate: relationship to complexation in solution, *Food Hydrocolloids*, 2008, **22**, 647-659.

39. Q. Li, T. Li, C. Liu, J. Chen, R. Zhang, Z. Zhang, T. Dai and D. J. McClements, Potential physicochemical basis of Mediterranean diet effect: Ability of emulsified olive oil to increase carotenoid bioaccessibility in raw and cooked tomatoes, *Food Research International*, 2016, **89**, 320-329.

40. Z. Zhang, R. Zhang, L. Zou and D. J. McClements, Tailoring lipid digestion profiles using combined delivery systems: mixtures of nanoemulsions and filled hydrogel beads, *RSC Advances*, 2016, **6**, 65631-65637.

41. C. J. F. Souza and E. E. Garcia-Rojas, Effects of salt and protein concentrations on the association and dissociation of ovalbumin-pectin complexes, *Food Hydrocolloids*, 2015, **47**, 124-129.

42. D. J. McClements and Y. Li, Structured emulsion-based delivery systems: Controlling the digestion and release of lipophilic food components, *Advances in colloid and interface science*, 2010, **159**, 213-228.

43. Q. Li, T. Li, C. M. Liu, T. T. Dai, R. J. Zhang, Z. P. Zhang and D. J. McClements, Enhancement of Carotenoid Bioaccessibility from Tomatoes Using Excipient Emulsions: Influence of Particle Size, *Food Biophysics*, 2017, **12**, 172-185.

44. E. Dickinson, M. G. Semenova, A. S. Antipova and E. G. Pelan, Effect of high-methoxy pectin on properties of casein-stabilized emulsions, *Food Hydrocolloids*, 1998, **12**, 425-432.

45. D. J. McClements, Theoretical analysis of factors affecting the formation and stability of multilayered colloidal dispersions, *Langmuir*, 2005, **21**, 9777-9785.

46. F. Yasumaru and D. Lemos, Species specific in vitro protein digestion (pH-stat) for fish: method development and application for juvenile rainbow trout (Oncorhynchus mykiss), cobia (Rachycentron canadum), and Nile tilapia (Oreochromis niloticus), *Aquaculture*, 2014, **426**, 74-84.

47. T. K. Singh, S. K. Øiseth, L. Lundin and L. Day, Influence of heat and shear induced protein aggregation on the in vitro digestion rate of whey proteins, *Food & Function*, 2014, **5**, 2686-2698.

48. J. M. Lattimer and M. D. Haub, Effects of Dietary Fiber and Its Components on Metabolic Health, *Nutrients*, 2010, **2**, 1266-1289.

49. I. J. P. Colle, S. Van Buggenhout, L. Lemmens, A. M. Van Loey and M. E. Hendrickx, The type and quantity of lipids present during digestion influence the in vitro bioaccessibility of lycopene from raw tomato pulp, *Food Research International*, 2012, **45**, 250-255.
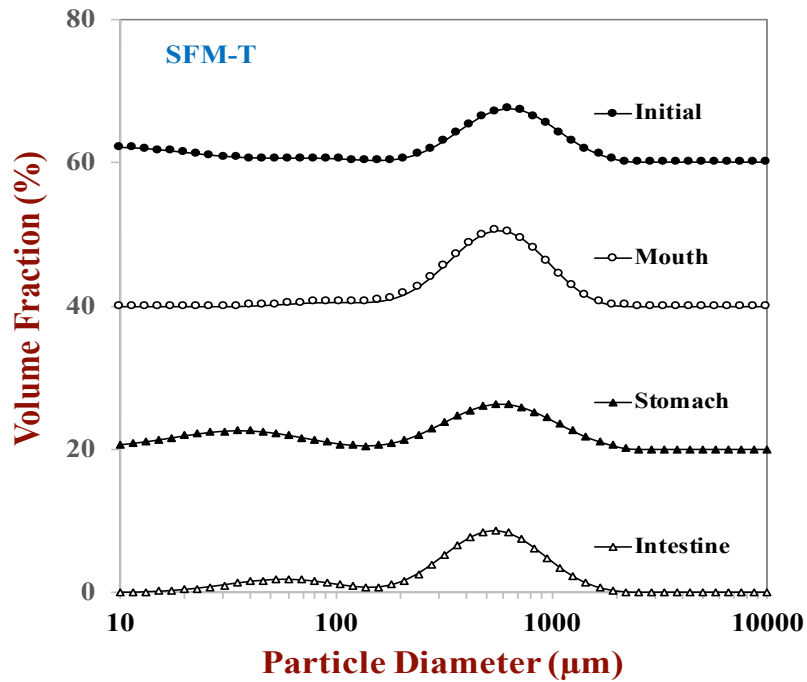
50.  I. J. P. Colle, L. Lemmens, S. Van Buggenhout, K. Met, A. M. Van Loey and M. E. Hendrickx, Processing tomato pulp in the presence of lipids: The impact on lycopene bioaccessibility, *Food Research International*, 2013, **51**, 32-38.
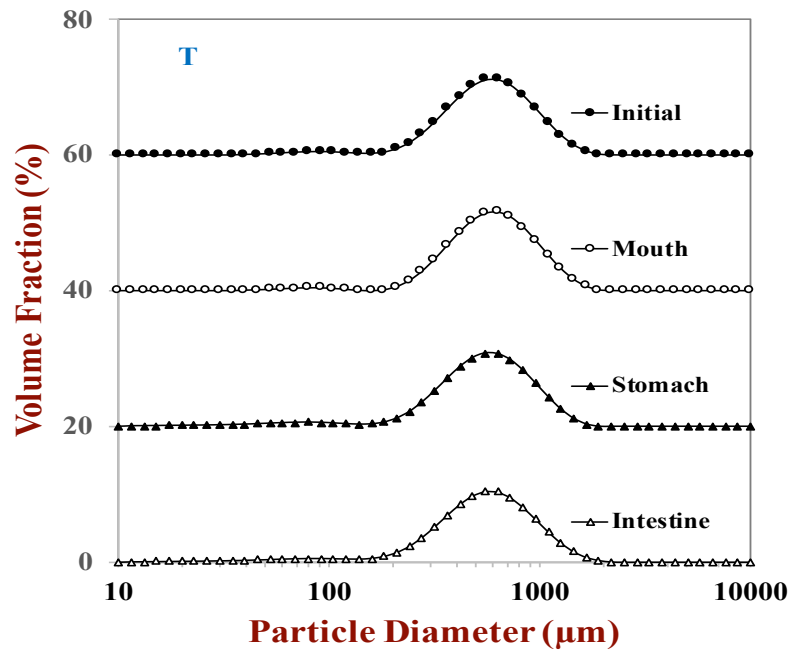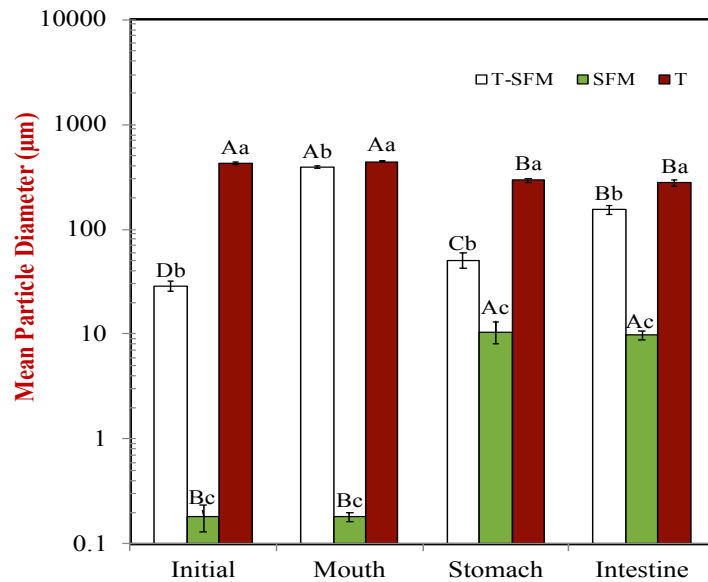
**(a)**
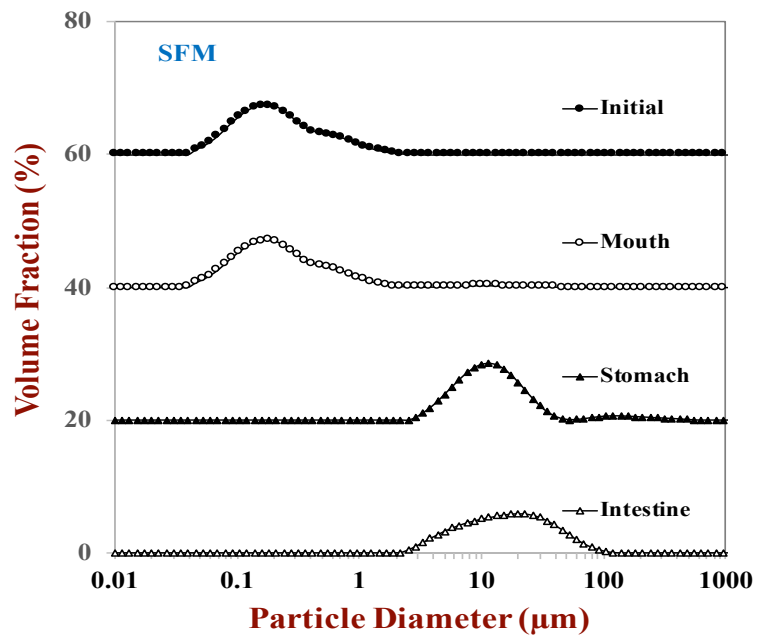


**(b)**

**(c)**



**(d)**

**Figure 1.** Particle size distributions of (a) raw tomato and (b) standardized food model (c) crushed tomato and (d) surface-weighted mean particle diameter ($d_{32}$) of all samples after exposure to successive GIT stage.
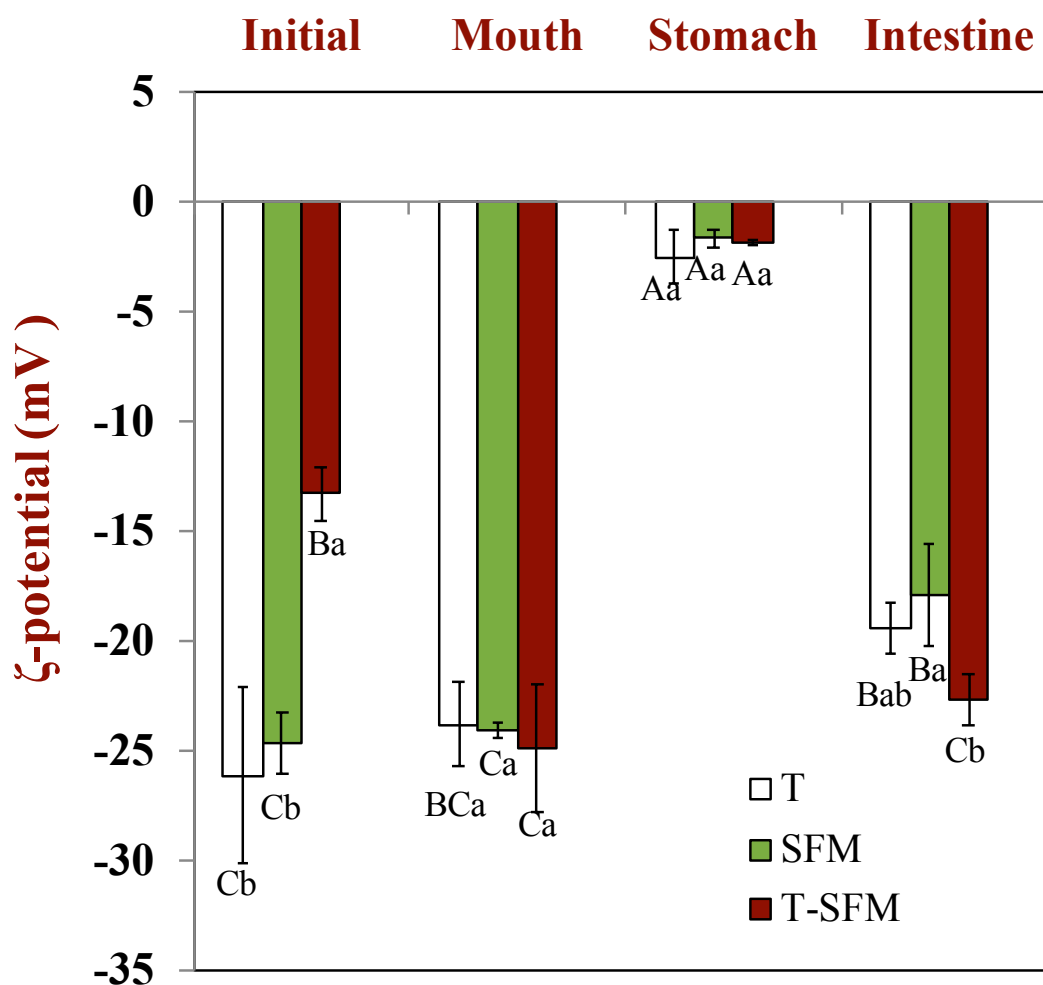
**Figure 2.** Electrical properties of the different samples measured after exposure to different GIT stages (T: crushed tomato; SFM: standardized food model; T-SM: crushed tomato with standardized food model). Samples designated with different capital letters (A, B, C, D) were significantly different (Duncan, $p < 0.05$) when compared between different GIT regions (same sample). Samples designated with different upper case letters (a, b, c) were significantly different (Duncan, $p < 0.05$) when compared between different samples (same GIT region).
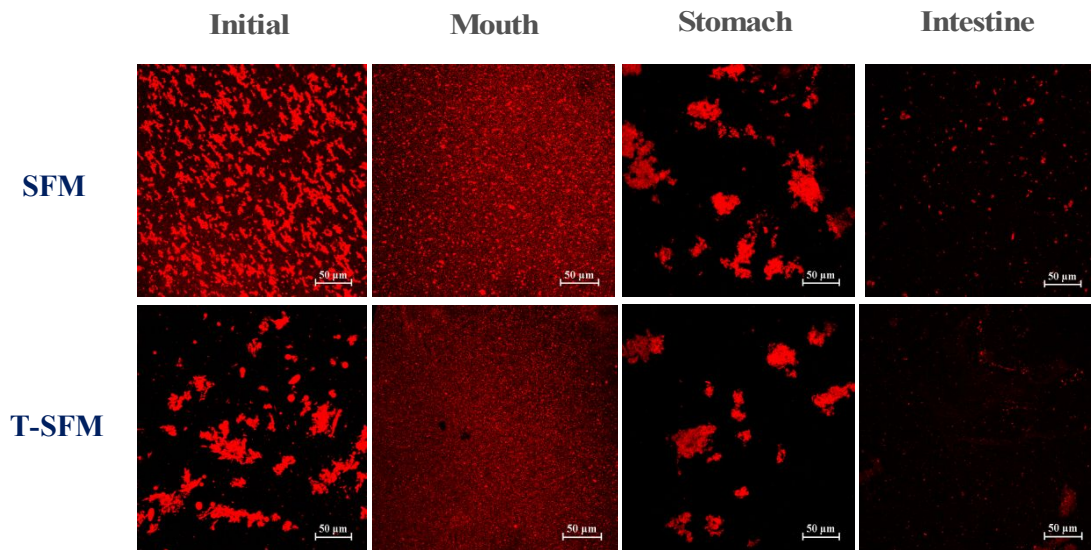
**Figure 3.** Microstructures of different samples after exposing to different regions of the simulated GIT (Scale bar is 50 μm). (SFM: standardized food model; T-SFM: crushed tomato with standardized food model)
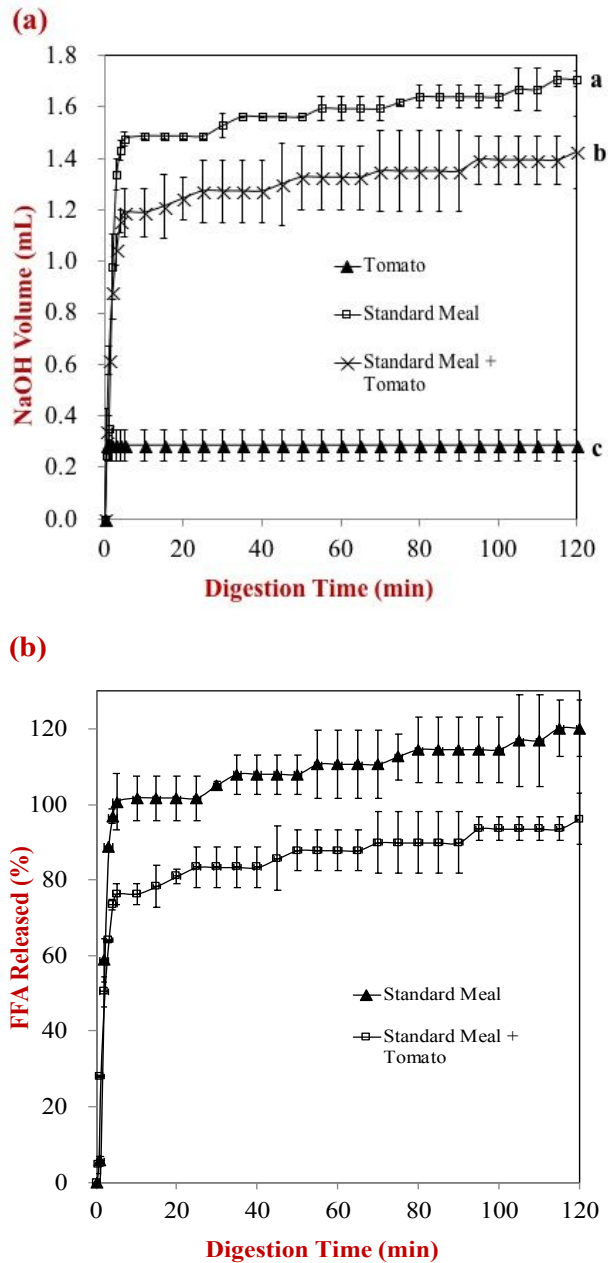
**(a)**



**(b)**



**Figure 4.** The digestion profiles of different samples under simulated intestinal digestion measured using a pH-stat *in vitro* digestion model. Samples designated with different capital letters (a, b and c) were significantly different (Duncan, $p < 0.05$) when compared between different delivery systems for the final point (120 min).
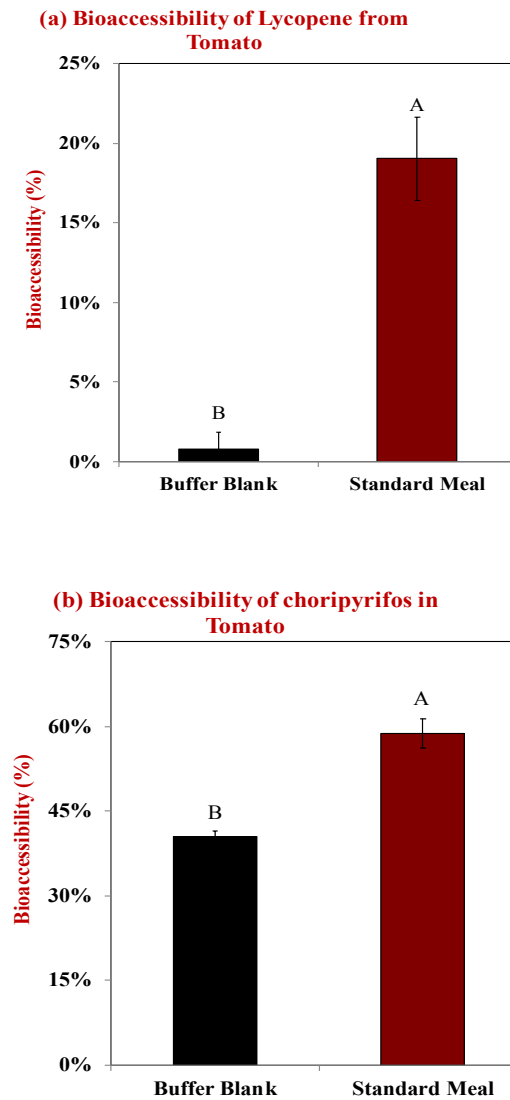
**(a) Bioaccessibility of Lycopene from Tomato**



**(b) Bioaccessibility of choripyrifos in Tomato**



**Figure 5.** Bioaccessibility of (a) lycopene and (b) choripyrifos in different delivery systems measured after exposure to simulated small intestine conditions（The lycopene concentration was determined by HPLC and the chlorpyrifos concentration in the samples was determined by measuring the intensity of the ^{14}C-radioactive signal using liquid scintillation counting). Samples designated with different capital letters (A, B) were significantly different (T. Test, $p < 0.05$) when compared between different treatments.

**Table 1:** The formulation of standardized food model based on the survey of the typical US diet (www.ars.usda.gov/nea/bhnrc/fsrg).

| Component | Level (g/100g) |
| --- | --- |
| Protein (Sodium caseinate) | 3.44 |
| Sugar (Sucrose) | 4.57 |
| Dietary Fiber (Pectin) | 0.70 |
| Starch (Corn starch) | 5.15 |
| Fat (Corn oil) | 3.42 |
| Minerals (Sodium chloride) | 0.534 |